

Statistical properties and attack tolerance of growing networks with algebraic preferential attachment

Zonghua Liu,¹ Ying-Cheng Lai,^{1,2} and Nong Ye³¹*Department of Mathematics, Center for Systems Science and Engineering Research, Arizona State University, Tempe, Arizona 85287*²*Department of Electrical Engineering and Physics, Arizona State University, Tempe, Arizona 85287*³*Department of Industrial Engineering, Department of Computer Science and Engineering, Arizona State University, Tempe, Arizona 85287*

(Received 13 May 2002; published 16 September 2002)

We consider growing networks with algebraic preferential attachment and address two questions: (1) what is the effect of temporal fluctuations in the number of new links acquired by the network? and (2) what is the network tolerance against random failures and intentional attacks? We find that the fluctuations generally have little effect on the network properties, although they lead to a plateau behavior for small degrees in the connectivity distribution. Formulas are derived for the evolution and distribution of the network connectivity, which are tested by numerical simulations. Numerical study of the effect of failures and attacks suggests that networks constructed under algebraic preferential attachment are more robust than scale-free networks.

DOI: 10.1103/PhysRevE.66.036112

PACS number(s): 84.35.+i, 89.75.Hc, 02.50.Cw, 05.40.-a

I. INTRODUCTION

There has been an increasing interest in large, evolving complex networks [1] since the seminal papers on scale-free networks [2] and on small-world networks [3]. In general, networks in nature may or may not possess an organized structure in the following sense. There are networks with a hierarchy of structures in that the number of links of various nodes follows a power-law (or an algebraic) probability distribution. These are called scale-free networks [2]. More specifically, let $P(k)$ be the connectivity distribution, where k is the realization of a random variable K measuring the number of links at a node. Scale-free networks are characterized by

$$P(k) \sim k^{-\gamma}, \quad (1)$$

where $\gamma > 0$ is the algebraic scaling exponent. Because of the algebraic distribution, typically there are nodes in the network with a relatively large numbers of links, and these can be key to efficient functioning of the network. In random networks [4], nodes are connected to each other in a completely random fashion and as such there exists no apparent structure. The connectivity distribution for random networks are typically exponential: $P(k) \sim \exp(-ak)$, where $a > 0$ is a constant. We note that the small-world concept describes the fact that the average path between any two nodes in a large network can be relatively short. In the small-world network model proposed by Watts and Strogatz [3], $P(k)$ is assumed to be exponential. The small-world feature appears to be universal for large, sparse networks, regardless of whether they have an underlying organized structure. In fact, the pioneering study on random graphs by Erdős and Rényi already indicated that the typical distance between any two nodes scales logarithmically with the number of nodes [4] and many apparently scale-free networks are small world, too [1].

The mechanisms leading to the algebraic connectivity distribution in scale-free networks are argued to be growth and preferential attachment [2,5], where the former means that the size of the network keeps increasing with time and the

latter assumes that the relative probability for an already heavily connected node to get new links is proportionally large. In particular, at a given time the probability Π_i for a node in the network with k links to acquire a new link is assumed to be [2,5]

$$\Pi_i \sim k. \quad (2)$$

This form of preferential-attachment rule yields the universal scaling exponent $\gamma=3$ [2,5]. [We note that for random networks, $\Pi(k)$ is constant.] While many realistic networks in nature are scale-free to some extent, the fitted algebraic scaling exponents typically deviate from the ideal value of 3 [2,5], which prompts the study of various related models for scale-free networks [6–16]. Another issue of concern is that there are examples where the distribution is neither power law nor exponential, such as the scientific collaboration network [17]. These mean that, for a realistic network, the attachment probability $\Pi(k)$ is neither linear (as in the case of idealized scale-free networks) nor constant (as in random networks). A natural way to generalize is then to consider the following form of algebraic preferential-attachment probability [6,18]:

$$\Pi_i \sim k^\alpha, \quad (3)$$

where $0 \leq \alpha \leq 1$ is the algebraic exponent.

Network properties resulted from the attachment rule (3) are the subject of this paper. Our motivations are two.

(a) In existing works with Eq. (3), the effect of random fluctuations has not been considered. For example, when new nodes are added to the network at different times, the number of new links is generally not constant. A question is then how this type of fluctuations affect the network topology as characterized by the connectivity distribution $P(k)$.

(b) The issue of robustness against random failures or intentional attacks for networks described by the attachment rule (3) is important but, to our knowledge, it has not been studied. In this regard, resilience of a network under failures or attacks can be conveniently characterized by how the di-

ameter [19] of the network is changed [20,21], which is the average length of the shortest paths between any two nodes in the network.

The principal results of this paper are as following: (1) under random fluctuations the connectivity distribution $P(k)$ tends to develop a plateau for small values of k , and (2) networks with algebraic attachment exponent around the value of 0.5 are relatively robust against intentional attacks, while still possessing a significant component of organized structures. We derive theoretical formulas and provide numerical support to establish our results, which can be useful not only for better understanding of realistic complex networks but also for designing secure, robust engineering networks.

In Sec. II, we derive the connectivity distribution $P(k)$ under algebraic attachment rule (3) in the presence of random link fluctuations and provide numerical support. In Sec. III, we address to what extent the network is affected by random failures and intentional attacks. A discussion is presented in Sec. IV.

II. CONNECTIVITY DISTRIBUTION AND EFFECT OF LINK FLUCTUATIONS

Our model is described as follows. Starting with a small number (m_0) of nodes, we add a new node with m edges (or links) at each time step to the network. Since we allow for fluctuations in m , we write $m(t)$. Each link is chosen according to the following attachment probability Π_i :

$$\Pi_i = \frac{k_i^\alpha}{\sum_j k_j^\alpha}, \quad (4)$$

where the summation is over the whole network at a given instant, α is a constant in $[0,1]$, and $m(t)$ is a random number chosen from $\{1,2,\dots,2\bar{m}-1\}$ with the average value \bar{m} . In the first m_0-1 steps, we limit $m(t) \leq m_0+t-1$ to guarantee that the number of new links does not exceed the number of nodes in the network in this initial time interval. Our model reduces to that in Ref. [6] if $m(t)$ is constant. Figure 1 shows, schematically, the process of adding new nodes to the network for $m_0=3$ and $\bar{m}=3$.

To derive the connectivity distribution $P(k)$, we first consider the case with no fluctuations where $m(t)=\bar{m}$ and use the mean-field approach proposed in Ref. [2]. For a large network, the random variable K is approximately continuous and the attachment probability Π_i can be regarded as the continuous rate of change of k_i . We have

$$\frac{\partial k_i}{\partial t} = \bar{m} \Pi_i(k_i) = \frac{\bar{m} k_i^\alpha}{\sum_j k_j^\alpha}. \quad (5)$$

Because $\sum_j k_j^0 = t$ and $\sum_j k_j^1 = 2\bar{m}t$, where t is the evolution time, we have

$$\sum_j k_j^\alpha = \mu t \text{ and } 1 < \mu < 2\bar{m} \text{ for } 0 < \alpha < 1 \quad (6)$$

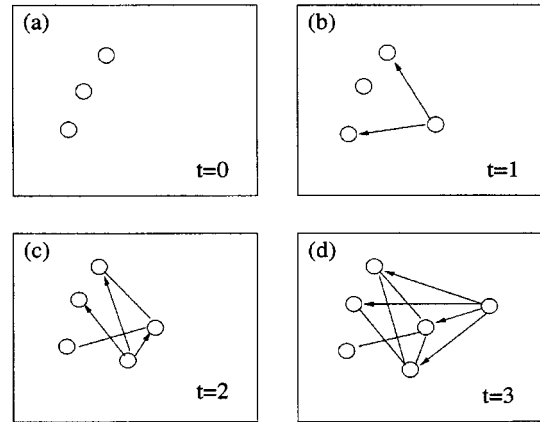


FIG. 1. Schematic illustration of how a network grows in algebraic preferential-attachment model with link fluctuations for $m_0 = \bar{m} = 3$. At $t=0$ the system has $m_0=3$ isolated nodes. At $t=1$ a new node and two links are added. At $t=2$ a new node and three links are added. At $t=3$ a new node and four links are added, and so on.

because $\sum_j k_j^0 < \sum_j k_j^\alpha < \sum_j k_j^1$. Substituting Eq. (6) into Eq. (5) yields

$$\frac{\partial k_i}{\partial t} = \frac{\bar{m} k_i^\alpha}{\mu t}. \quad (7)$$

Note that the above derivation does not yield μ , the time-rate change of the quantity $\sum_j k_j^\alpha$ which, however, can be computed numerically. Intuitively, μ increases with α , as shown in Fig. 2 for $m(t)=\bar{m}=5$. The appendix lists our procedure for computing the $\mu - \alpha$ relation. The general observation is that μ is a monotonically increasing function of α .

Integrating Eq. (7) under the initial condition: $k_i(t_i) = \bar{m}$, we obtain

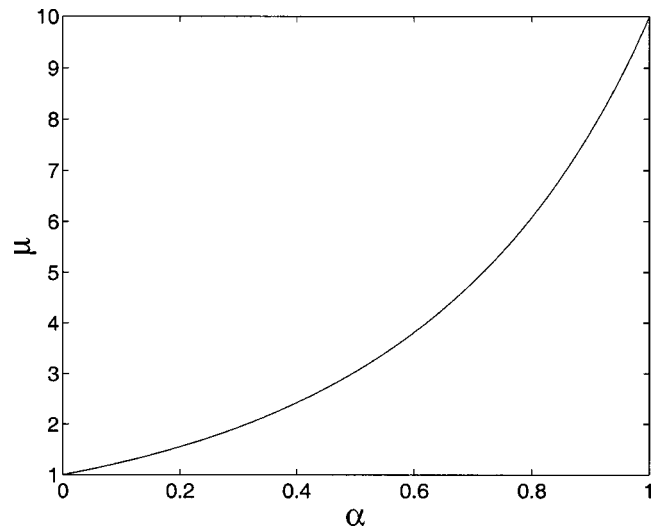


FIG. 2. Numerically obtained time-rate change μ of $\sum_j k_j^\alpha$ versus α for $m(t)=\bar{m}=5$.

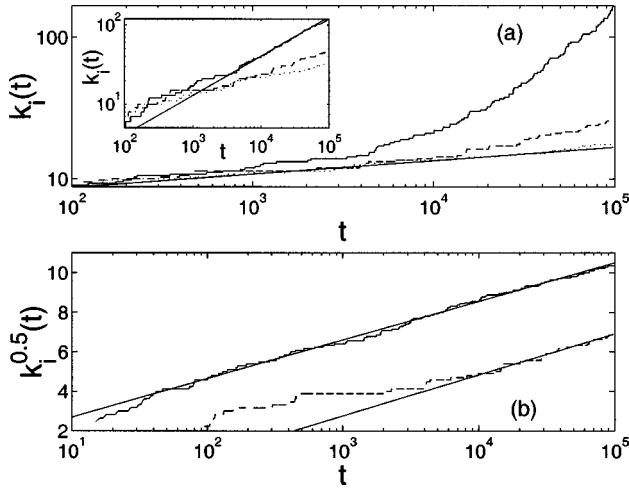


FIG. 3. Temporal evolution of the connectivity $k_i(t)$ of a typical node with $m_0 = \bar{m} = 5$ in the network for the specific case $m(t) = \bar{m}$. (a) Cases of different α where the solid, dashed, and dotted curves are for $\alpha = 1$, $\alpha = 0.5$, and $\alpha = 0$, respectively. The node is added to the network at $t_i = 95$. The inset plots the same data but on a logarithmic scale. (b) Cases of different initial time with $\alpha = 0.5$, where the solid and dashed curves are for nodes added to the network at $t = 15$ and $t = 95$, respectively.

$$k_i(t)^{1-\alpha} = \bar{m}^{1-\alpha} + \ln\left(\frac{t}{t_i}\right)^{(1-\alpha)(\bar{m}/\mu)} \sim (1-\alpha) \frac{\bar{m}}{\mu} \ln t \text{ for } 0 \leq \alpha < 1. \quad (8)$$

For $\alpha = 0$, α approaches 1, and Eq. (8) becomes $k_i(t) \sim \bar{m} \ln t$ and $k_i(t) \sim \sqrt{t}$, respectively. Figure 3(a) shows the results of numerical simulation, where $k_i(t)$ versus $\ln t$ is plotted for $\bar{m} = m_0 = 5$ and $t_i = 95$. In the figure, the solid, the dashed, and the dotted curves denote the cases where $\alpha = 1$ (scale-free network), $\alpha = 0.5$ (mixed network), and $\alpha = 0$ (random network), respectively. For $\alpha = 0$, $k_i(t)$ appears to be proportional to $\ln t$. A least-squares fit of the $\alpha = 0$ line gives the slope of 11.0 (approximately), which agrees very well with the prediction (8). For $\alpha = 1$, $k_i(t)$ is algebraic, as can be seen in the inset where $k_i(t)$ is plotted on a logarithmic scale. We find that the algebraic exponent is approximately 0.5, which was the case for scale-free networks with linear preferential attachment [5]. For $0 < \alpha < 1$, Eq. (8) predicts that $k_i(t)^{1-\alpha}$ scales linearly with $\ln t$ with the slope $(1-\alpha)\bar{m}/\mu$ [or with $\log_{10}(t)$ with the slope reduced by $\ln 10$] independent of the value of t_i . Figure 3(b) shows, for $\alpha = 0.5$, $k_i(t)^{1-\alpha}$ versus $\log_{10} t$ for two nodes added to the network at $t_i = 15$ (solid curve) and $t_i = 95$ (dashed curve), where the numerical slope of about 1.92 is approximately the same for both cases, which agrees with Eq. (8).

The connectivity distribution can be derived from Eq. (8). The probability that a node has a connectivity $k_i(t)$ smaller than k , $P(k_i(t) < k)$ can be written as

$$P(k_i(t) < k) = P\left[t_i > t \exp\left(-\frac{k^{1-\alpha} - \bar{m}^{1-\alpha}}{1-\alpha} \frac{\mu}{\bar{m}}\right)\right]. \quad (9)$$

Assuming that nodes are added to the network at equal time intervals, the probability density of t_i is $P_i(t_i) = 1/(m_0 + t)$. Substituting this into Eq. (9) yields

$$\begin{aligned} & P\left[t_i > t \exp\left(-\frac{k^{1-\alpha} - \bar{m}^{1-\alpha}}{1-\alpha} \frac{\mu}{\bar{m}}\right)\right] \\ &= 1 - P\left[t_i \leq t \exp\left(-\frac{k^{1-\alpha} - \bar{m}^{1-\alpha}}{1-\alpha} \frac{\mu}{\bar{m}}\right)\right] \\ &= 1 - \frac{t}{m_0 + t} \exp\left(-\frac{k^{1-\alpha} - \bar{m}^{1-\alpha}}{1-\alpha} \frac{\mu}{\bar{m}}\right). \end{aligned} \quad (10)$$

The probability density $P(k)$ can be obtained using

$$\begin{aligned} P(k) &= \frac{\partial p(k_i(t) < k)}{\partial k} \\ &= \frac{t}{m_0 + t} \frac{\mu}{\bar{m}} k^{-\alpha} \exp\left(-\frac{k^{1-\alpha} - \bar{m}^{1-\alpha}}{1-\alpha} \frac{\mu}{\bar{m}}\right). \end{aligned} \quad (11)$$

We see that $P(k)$ is generally a mixture of both algebraic and exponential distributions. For $\alpha = 0$, we have

$$P(k) \sim \exp\left(-\frac{k}{\bar{m}}\right),$$

which is exponential. When α approaches unity, we have

$$\lim_{\alpha \rightarrow 1} \frac{k^{1-\alpha} - \bar{m}^{1-\alpha}}{1-\alpha} = \ln k - \ln \bar{m},$$

which, by Eq. (11), gives

$$P(k) = \frac{2\bar{m}^2}{m_0 + t} \frac{1}{k^3}.$$

This is the connectivity distribution for idealized scale-free networks. Note that here, Eq. (11) is a general expression for all values of α in $[0, 1)$, whereas Ref. [14] gives different expressions for different values of α .

Figure 4(a) shows the numerically computed connectivity distribution $P(k)$ with $m(t) = \bar{m} = m_0 = 5$ for different α values, where the open circles, the stars, and the squares denote cases of $\alpha = 1$, $\alpha = 0.5$, and $\alpha = 0$, respectively. We see that the distribution is clearly algebraic for $\alpha = 1$, whereas a plot on a semilogarithmic scale indicates that the distribution for $\alpha = 0$ is exponential. The distribution for $\alpha = 0.5$ lies somewhere in between these two cases, indicating a mixture of algebraic and exponential components in $P(k)$. Figure 4(b) shows for $\alpha = 0.5$ the distributions for different values of \bar{m} on a semilogarithmic scale, where the open circles, the stars, and the squares denote the cases where $\bar{m} = m_0 = 3$, $\bar{m} = m_0$

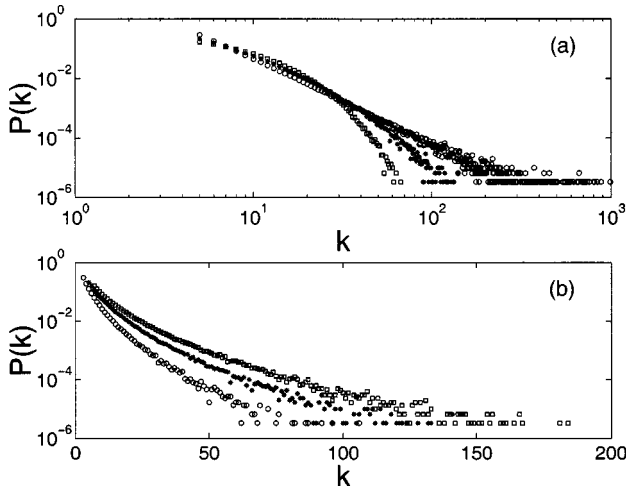


FIG. 4. Connectivity distribution $P(k)$ for the specific case $m(t) = \bar{m}$. (a) Cases of different α with $m_0 = \bar{m} = 5$, where the open circles, stars, and squares denote $\alpha = 1$, $\alpha = 0.5$, and $\alpha = 0$, respectively. For $\alpha = 1$, the scaling is clearly a power law, with deviations from it as α is decreased. (b) Cases of different \bar{m} with $\alpha = 0.5$, where the open circles, the stars, and the squares denote $\bar{m} = m_0 = 3$, $\bar{m} = m_0 = 5$, and $\bar{m} = m_0 = 7$, respectively.

$= 5$, and $\bar{m} = m_0 = 7$, respectively. All these distributions are neither completely algebraic nor exponential.

We now consider the case where there are fluctuations in $m(t)$. For convenience, we write $m(t)$ in terms of a new random variable $\xi(t)$,

$$m(t) = \bar{m}[1 + \xi(t)], \quad (12)$$

where $\bar{m}[1 + \xi(t)] = \{1, 2, \dots, 2\bar{m} - 1\}$ and $\langle \xi(t) \rangle = 0$. Following the steps leading to $k_i(t)$ and $P(k)$ for the constant m case, we obtain

$$k_i(t)^{1-\alpha} = \bar{m}^{1-\alpha} [1 + \xi(t)] + \ln \left(\frac{t}{t_i} \right)^{(1-\alpha)(m_t/\mu)} \\ \sim (1-\alpha) \frac{m_t}{\mu} \ln t \quad \text{for } 0 \leq \alpha < 1, \quad (13)$$

and

$$P(k) = \frac{t}{m_0 + t} \frac{\mu}{m_t} k^{-\alpha} \exp \left(- \frac{k^{1-\alpha} - \bar{m}^{1-\alpha} [1 + \xi(t)]}{1-\alpha} \frac{\mu}{m_t} \right), \quad (14)$$

where m_t is a random number in between 1 and $2\bar{m} - 1$ and is defined by

$$m_t \ln(t) = \int_{t_i}^{t} \frac{\bar{m}[1 + \xi(t)]}{t} dt.$$

As $t \rightarrow \infty$, $m_t \rightarrow \bar{m}$. This indicates that at large times, $k_i(t)$ and $P(k)$ should exhibit similar behaviors to those for the constant m cases. Figure 5 shows the numerical results of $k_i(t)$, where the figure legends are the same as in Fig. 3. The

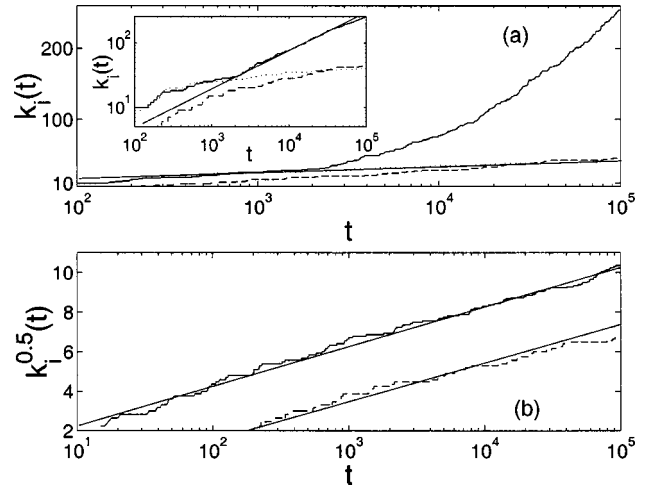


FIG. 5. Evolution of the connectivity $k_i(t)$ of a typical node in a network with fluctuations in m , where $m_0 = \bar{m} = 5$. (a) $k_i(t)$ versus $\log_{10} t$ for different values of α . The node is added to the system at $t = 95$. The solid, the dashed, and the dotted curves are for $\alpha = 1$, $\alpha = 0.5$, and $\alpha = 0$, respectively. The inset is $\log_{10} k_i(t)$ versus $\log_{10} t$. (b) For $\alpha = 0.5$, $k_i^{0.5}(t)$ versus $\log_{10} t$ for two nodes added to the network at $t = 15$ and $t = 95$, respectively.

slopes of the linear fit in the inserts of Fig. 5(a) and of those in Fig. 5(b) agree with the theoretical predictions very well. Figure 6 shows the connectivity distribution $P(k)$, where the legends are the same as those in Fig. 4. The behaviors of $P(k)$ for $k > 10$ for different values of α are similar to those observed in the corresponding constant m cases, as predicted by Eq. (14).

Comparing Figs. 5 and 6 with Figs. 3 and 4, respectively, we observed that having fluctuations in $m(t)$ only affects the structure of the network for small values of k . In particular, there appears to be a plateau region in $P(k)$ for $k \leq 10$, which can be understood heuristically as follows. For the case where m is constant, the distribution $P(k)$ starts from a minimum value $k_{min} = m$. When $m(t)$ fluctuates in the range $[1, m_{max}]$, statistically $P(k)$ can start for all k values in this range with approximately equal probabilities, giving rise to the plateau behavior. We note that many realistic networks such as the world-wide-web [19], the actor-collaboration network [2], and the scientific-citation network [17] indeed exhibit an approximate plateau region in $P(k)$ for small k values.

III. ATTACK TOLERANCE

We now investigate the effect of random failure and intentional attack on the general networks. Here failure means random removal of a fraction of nodes and attack means targeted destruction of some critical nodes such as the heavily connected ones in the network. The recent study by Albert *et al.* [20] indicates that the growing networks with exponentially distributed connectivity are robust against both intentional attacks and random removals of a relatively small fraction of nodes. Scale-free networks, on the other hand, appear to be robust against random failures but are more sensitive to intentional attacks. This is somewhat expected

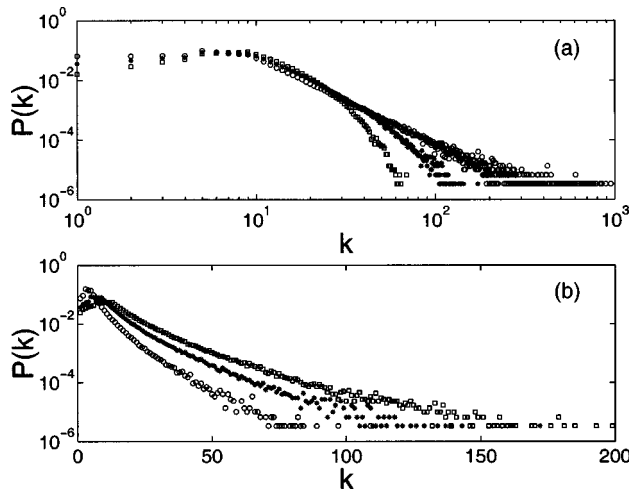


FIG. 6. The connectivity distribution $P(k)$ for a network with fluctuations in m . (a) $P(k)$ versus K on a logarithmic scale, where the open circles, the stars, and the squares denote the cases of $\alpha = 1$, $\alpha = 0.5$, and $\alpha = 0$, respectively. Other network parameters are $m_0 = \bar{m} = 5$. For $\alpha = 1$, the scaling is algebraic for $k \geq 10$. For $\alpha = 0$, the scaling appears to be exponential for $k \geq 10$. (b) For $\alpha = 0.5$, $P(k)$ versus k on a semilogarithmic scale, where the open circles, the stars, and the squares denote cases of $\bar{m} = m_0 = 3$, $\bar{m} = m_0 = 5$, and $\bar{m} = m_0 = 7$, respectively.

because a scale-free network typically possesses a few heavily connected, or “center” nodes. Attack on these nodes would have a significant impact on the performance of the network.

To quantify the robustness of a network against random failures or attacks, Albert *et al.* suggested [20] using the concept of *diameter* [19], which is the average number of links between any two nodes in the network, a concept that is similar to the average shortest path in the small-world characterization of networks [3]. Computation of the diameter requires searching through all pairs of nodes in the network, which is numerically intensive when the size of the network is large [17]. We have thus developed a simple method to compute the diameter D of a large network, which is numerically efficient. Specifically, at a given time, we randomly choose n nodes from the network so that an increase in n does not result in appreciable variations in D . For each node, we regard it as a center and assign the number 1 to its nearest neighbor, 2 to its second nearest neighbors, and so on until all nodes are assigned a number. The average of all these numbers give the distance d_1 from the “center” node to an arbitrary node. Choosing the center node in turn yields an additional $(n-1)$ distances d_i ($i=2, \dots, n$). The diameter D is taken to be the average value of the n distances.

Figure 7 shows, for a network constructed according to the algebraic preferential-attachment rule (4) at a time when there are 10^4 nodes, the diameter D versus the algebraic parameter α , where the solid and the dashed curves correspond to cases of constant and fluctuating m , respectively. There is little difference between the two curves, indicating that fluctuations in the number of links have negligible effect on the efficiency of the network. As α is increased from zero, D

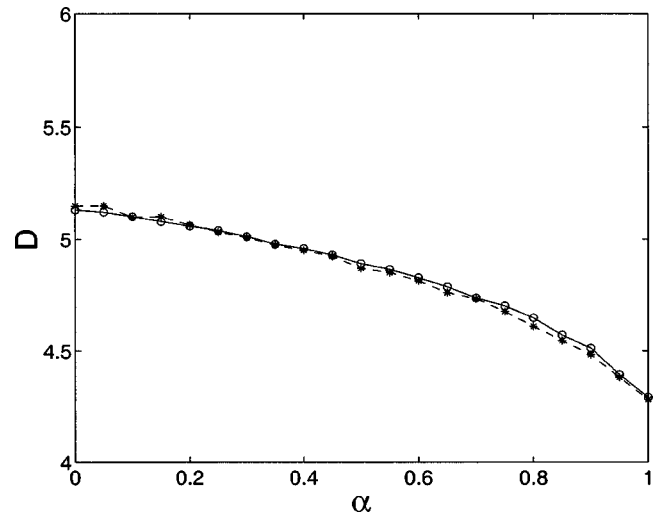


FIG. 7. Diameter versus the parameter α with $m_0 = \bar{m} = 3$, where the solid and dashed lines denote the constant and fluctuating m cases, respectively.

tends to decrease, indicating that with respect to “communication,” networks with heavier scale-free components are slightly more efficient as compared with a random networks. Overall, the value of D remains small for $0 \leq \alpha \leq 1$, suggesting that networks developed according to Eq. (4) are all small world, regardless of whether they are random or scale-free, or a mixture of both.

We now present results concerning the effect of random failures and attacks. Figure 8 shows, for a network consisting of 10^4 nodes grown from $\bar{m} = m_0 = 3$, its diameter versus the fraction f of the randomly failing nodes, where Figs. 8(a) and 8(b) are for constant and fluctuating m , respectively, and open circles, stars, and squares denote networks with $\alpha = 1$, $\alpha = 0.5$, and $\alpha = 0$, respectively. Apparently, as f is increased, the diameters increase in a similar manner for all networks considered, regardless of whether they are random or scale-free, with or without fluctuations in m . Note that for all cases, the diameter is increased about 4% even when 10% of the nodes in the network fail. This indicates that random failures have similar but small effect on the class of growing networks developed according to the algebraic attachment rule (4). Note, however, that the absolute values of the diameter for a random network are larger than those of scale-free and mixed networks.

For intentional attacks, the situation changes completely. Figure 9 shows, for the same network as in Fig. 8, the diameter versus the fraction f of intentionally removed nodes with largest numbers of links, where panels Figs. 9(a) and 9(b) are for constant and fluctuating m , respectively. The open circles, the stars, and the open squares denote the $\alpha = 1$ (scale-free), $\alpha = 0.5$ (mixed), and $\alpha = 0$ (random) cases, respectively. We observe that networks grown with different values of α exhibit distinct behaviors. In particular, the diameter for scale-free networks (open circles) increases more rapidly as f is increased, compared with mixed (stars) and random (open squares) networks, indicating that scale-free networks are more vulnerable under attacks. For a mixed network, under

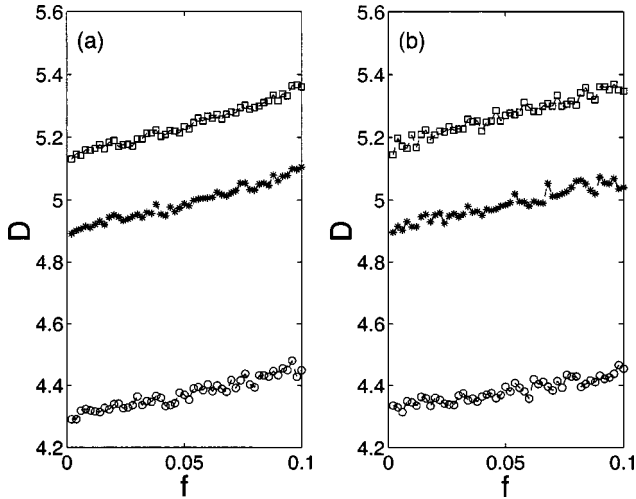


FIG. 8. Changes in the diameter D as a function of the fraction f of randomly removed nodes with $m_0 = \bar{m} = 3$, where (a) and (b) are for constant and fluctuating m , respectively. The open circles, the stars, and the open squares denote the $\alpha = 1$, $\alpha = 0.5$, and $\alpha = 0$ cases, respectively.

attacks its diameter increases only slightly more as compared with a random network. Again, whether there are fluctuations in m as the network grows has little effect on its performance under attacks.

The practical implications of these results are the following. Suppose one wishes to design a network with organized structures such as a set of “center” nodes, which should also be robust against attacks. The network cannot be random because of the structure requirement, but scale-free network is not desirable either, because of its vulnerability under at-

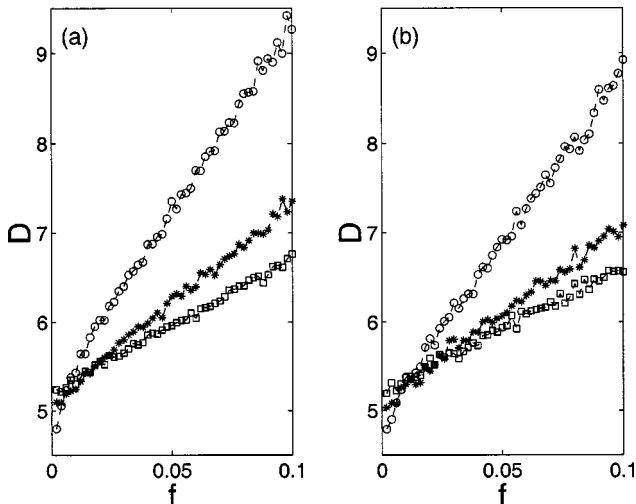


FIG. 9. Changes in the diameter D as a function of the fraction f of removed nodes with largest numbers of links in the network (attacks). The link parameter is $m_0 = \bar{m} = 3$. (a) and (b) are for constant and fluctuating m , respectively. The open circles, the stars, and the open squares denote the $\alpha = 1$ (scale-free), $\alpha = 0.5$ (mixed), and $\alpha = 0$ (random) cases, respectively. Apparently, scale-free networks are vulnerable under attacks, because the corresponding diameter increases most rapidly as f is increased.

tacks. Figure 9 suggests that mixed network with α around the value of 0.5 may be desirable because it allows for a significant proportion of organized structures at the same time, and is relatively robust against attacks.

IV. CONCLUSIONS

We have investigated a class of general growing networks with algebraic preferential-attachment rule. We focus on the evolution and statistical distribution of the connectivity, the effect of random fluctuations in the growing links, and the efficiency of the network under random failures and intentional attacks. Our conclusions are (i) random fluctuations in the links can cause a plateau behavior in the connectivity distribution $P(k)$ for small values of k , but otherwise they have little effect on the statistical properties of the network; (ii) mixed networks tend to be more robust against attacks as compared with scale-free networks. Since mixed networks still allow for a significant component of organized structures (versus random networks that do not), our conclusion (ii) may be important for the practical design of large scale networks that require structures such as “command” centers with relatively large numbers of links.

ACKNOWLEDGMENT

This work was supported by AFOSR under Grant No. F49620-01-1-0317.

APPENDIX

To obtain the relationship between the parameters μ and α , we use the method of master equation. Assuming that the average number of nodes with k links is $N_k(t)$, the master equation is

$$\frac{dN_k}{dt} = \frac{\bar{m}}{\sum_{j \geq m} j^\alpha N_j} [(k-1)^\alpha N_{k-1} - k^\alpha N_k] + \delta_{km} \bar{m}, \quad (\text{A1})$$

where $\sum_{j \geq m} j^\alpha N_j = \mu t$, the first term and second terms in the square bracket, and the δ -function term on the right-hand side of the equation represent the increase from the nodes originally with $k-1$ links, decrease from nodes original with k links, and increase due to new nodes, respectively. Write $N_k = t n_k$ [14], we obtain

$$n_k = \frac{\bar{m}}{\mu} [(k-1)^\alpha n_{k-1} - k^\alpha n_k]. \quad (\text{A2})$$

Solving Eq. (A2) and summing all the n_k yield

$$\frac{1}{\bar{m}} \sum_{k=m}^{\infty} \prod_{j=m}^k \left(1 + \frac{\mu}{m j^\alpha} \right)^{-1} = 1. \quad (\text{A3})$$

This equation can be used to numerically determine the relationship between μ and α , as shown in Fig. 2.

- [1] R. Albert and A.-L. Barabási, *Rev. Mod. Phys.* **74**, 47 (2002).
- [2] A.-L. Barabási and R. Albert, *Science* **286**, 509 (1999).
- [3] D.J. Watts and S.H. Strogatz, *Nature (London)* **393**, 440 (1998).
- [4] P. Erdős and A. Rényi, *Publ. Math. Inst. Hung. Acad. Sci.* **5**, 17 (1960); B. Bollobás, *Random Graphs* (Academic, London, 1985).
- [5] A.-L. Barabási, R. Albert, and H. Jeong, *Physica A* **272**, 173 (1999); **281**, 69 (2000).
- [6] P.L. Krapivsky, S. Redner, and F. Leyvraz, *Phys. Rev. Lett.* **85**, 4629 (2000).
- [7] S.N. Dorogovtsev, J.F.F. Mendes, and A.N. Samukhin, *Phys. Rev. Lett.* **85**, 4633 (2000); e-print cond-mat/0009090; e-print cond-mat/0011077.
- [8] R. Albert and A.-L. Barabási, *Phys. Rev. Lett.* **85**, 5234 (2000).
- [9] A. Vázquez, e-print cond-mat/006132; e-print cond-mat/0105031.
- [10] S.N. Dorogovtsev and J.F.F. Mendes, *Phys. Rev. E* **63**, 025101 (2001); **63**, 056125 (2001).
- [11] A.-L. Barabási, H. Jeong, E. Ravasz, Z. Nédá, A. Schubert, and T. Vicsek, e-print cond-mat/0104162.
- [12] G. Bianconi and A.-L. Barabási, *Europhys. Lett.* **54**, 436 (2001); *Phys. Rev. Lett.* **86**, 5632 (2001).
- [13] G. Ergün and G.J. Rodgers, e-print cond-mat/0103423.
- [14] P.L. Krapivsky and S. Redner, *Phys. Rev. E* **63**, 066123 (1999); P.L. Krapivsky, S. Redner, and F. Leyvraz, *Phys. Rev. Lett.* **85**, 4629 (2000).
- [15] P.L. Krapivsky, G.J. Rodgers, and S. Redner, *Phys. Rev. Lett.* **86**, 5401 (2001).
- [16] B. Tadić, *Physica A* **293**, 273 (2001); e-print cond-mat/0104029 (2001).
- [17] M.E.J. Newman, *Phys. Rev. E* **64**, 016132 (2001); B.J. Kim, C.N. Yoon, S.K. Han, and H. Jeong, *ibid.* **65**, 027103 (2002).
- [18] Another class of attachment rules that can generate networks with mixture of random and scale-free characteristics has recently been studied [Z. Liu, Y.-C. Lai, N. Ye, and P. Dasgupta, (unpublished)]. The model assumes that the attachment probability contains both a preferential and a random components, with a physical parameter controlling the relative weights between these components.
- [19] R. Albert, H. Jeong, and A.-L. Barabási, *Nature (London)* **401**, 130 (1999).
- [20] R. Albert, H. Jeong, and A.-L. Barabási, *Nature (London)* **406**, 378 (2000).
- [21] R. Cohen, K. Erez, D. Ben-Avraham, and S. Havlin, *Phys. Rev. Lett.* **85**, 4626 (2000); **86**, 3682 (2001).